On the generation process of upstream waves by a pressure distribution at critical speed

John Grue
Department of Mathematics, University of Oslo, Norway
johng@math.uio.no

1 Background and motivation

Wave effects from ships moving along shallow waterways continue to be of interest. The ship speed (U) relative to the shallow water speed ($c_0 = \sqrt{gh}$, g the acceleration of gravity, h the water depth), expressed by the Froude number ($Fr = U/c_0$), is typically subcritical ($Fr < 1$) but may in certain circumstances become critical ($Fr = 1$). This case is investigated here.

At subcritical speed, the waves due to high speed vessels ($Fr < 0.7$) in the Bay of Tallinn were measured, obtaining that a major part of the wave energy was due to components near the edge of the wave wake (Torsvik et al., 2015). Also at subcritical speed, conventional ships moving along the shallow waterways of Oslofjorden in Norway regularly generate an upstream mini-tsunami, where the wave generation occurs at the shallow depth changes of the water (Grue, 2017).

At critical speed ($Fr = 1$), water continuously piles up at the ship's bow. The wave energy spreads laterally. If the water is horizontally unbounded, a frontal system of three-dimensional, curved solitary waves is developed. This has been computed using nonlinear long wave theories such as the Kadomtsev-Petviashvili equation and variants of the Boussinesq equations, most notably by Lee and Grimshaw (1990) and Li and Sclavounos (2002). See also the references in these papers. If the motion takes place in a narrow channel, a sequence of long-crested solitary waves are formed (e.g., Wu, 1987). The big cruiseferries with a car-deck moving along the Oslofjorden may have a speed that for a short while is close to the shallow water speed. Questions concerning the upstream wave generation at $Fr = 1$ may be: What determines the incipient wavelength? How fast and strong is the process?

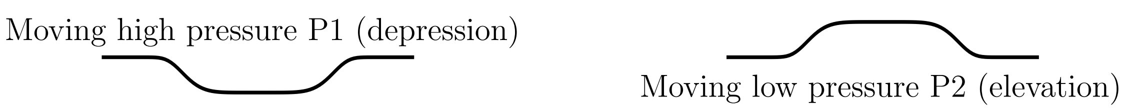

Figure 1: High P1 (low P2) pressure systems corresponding to depression (elevation).

We explore these questions by a set of fully dispersive and strongly nonlinear simulations. We combine simulations with two different moving pressure systems. One is a depression corresponding to a ship. This corresponds to a high pressure (Figure 1). We denote this by pressure system P1. This will generate a bow wave of elevation, and eventually a system of upstream three-dimensional solitons. A second pressure system is of elevation, of similar shape as the depression system, but where the draught is negative. This corresponds to a low pressure system. We denote this by pressure system P2. This has a negative bow wave, and there are no upstream waves. Instead, a long crested wave system fixed to the elevation pressure, of speed corresponding to $Fr = 1$ with a clearly defined wavelength develops. The wavelength defined by the P2-system is used as reference length of the waves of the P1-system (Figure 2).

2 Method

The fluid layer has constant depth h. A frame of reference is introduced. The driving pressure system (ship) is moving along the x-direction. Its position is $x_0(t)$, with $U = \dot{x}_0$. The vertical coordinate is y with $y = 0$ in the mean free surface. The lateral coordinate is z, and t is time. The moving surface pressure is specified by $P(x, z, t) = -\rho g Y_0(x - x_0, z)$ ($Y_0 < 0$).

Potential flow is assumed. The velocity potential is a superposition between a steady part with no waves (ϕ_0) plus an unsteady part representing the waves (ψ). ϕ_0 satisfies $(\partial\phi_0/\partial n)\sqrt{1 + |\nabla_1\zeta|^2} = V_0 = -U(\partial Y_0/\partial x)$ on $y = \zeta = Y_0 + \eta$ where η denotes the wave surface, $\partial/\partial n$ the normal derivative out of the fluid and ∇_1 the horizontal gradient. The rigid lid condition applies at $y = 0$ outside the region of the applied pressure, as well as at $y = -h$. Both potentials satisfy the Laplace equation in the fluid. Variable $v = (\partial\psi/\partial n)\sqrt{1 + |\nabla_1\zeta|^2}$, where $\partial\psi/\partial n$ is the normal derivative of ψ, is defined along the surface. The solution, obtained by an integral equation over the upper surface of the fluid, connects the potential and its normal derivative. The integral equation expressed in terms of Fourier transform over the horizontal plane (e.g., Grue, 2017) reads:

$$\hat{V}_0 + \hat{v} = kT\,(\hat{\phi}_0 + \hat{\psi}) + n.l.t.1, \tag{1}$$

where a hat denotes Fourier transform in the horizontal plane, $k = |(k_x, k_z)|$ the absolute value of the wavenumber vector in the Fourier domain, $T = \tanh(kh)$, and $n.l.t.1$ includes nonlinear contributions. The term $n.l.t.1$ is evaluated using two approximations including i) quadratic terms and ii) quadratic plus cubic terms, where results of the approximations are compared. The kinematic and dynamic boundary conditions at the wave surface are expressed in the Fourier transformed version:

$$\hat{\eta}_t - kT\,\hat{\psi} = n.l.t.1, \tag{2}$$

$$\hat{\psi}_t + g\hat{\eta} = U\mathbf{i}k_x\hat{\phi}_0 + n.l.t.2. \tag{3}$$

The term $U\mathbf{i}k_x\hat{\phi}_0$ in (3) contributes to the bow wave, and $n.l.t.2$ includes the (exact) nonlinear terms of the Bernoulli equation for the pressure.

3 Results

Simulations are carried out with the high pressure system P1 using $P_1 = -\rho g Y_0$ and with the low pressure system P2 using $P_2 = \rho g Y_0$, both with $Y_0 < 0$. The shape is given by $Y_0 = -d_0 \exp\Big(-[(x - x_0)/(l_0/2)]^6 - [z/(w_0/2)]^6\Big)$ where (l_0, w_0, d_0) denote the (length,width,draught). The dimensions of the big cruiseferries of Color Line are chosen with $l_0 = 210$ m, $w_0 = 35$ m and $d_0 = 6.8$ m, making a deplacement of 36 000 m^3. A water depth of $h = 14$ m is a realistic measure at a site where the mini-tsunami occurs. The numerical wave tank is $(L_x, L_z) = (250h, 250h)$. The resolution is $N_x = N_z = 760$ in each direction. The equations are integrated by a matlab script. Heun's method with $\Delta t = 0.2\sqrt{h/g}$ is used for the time integration. The integration is very robust. No smooting is applied. Products are anti-aliased in the Fourier domain. The simulations are fully dispersive and strongly nonlinear.

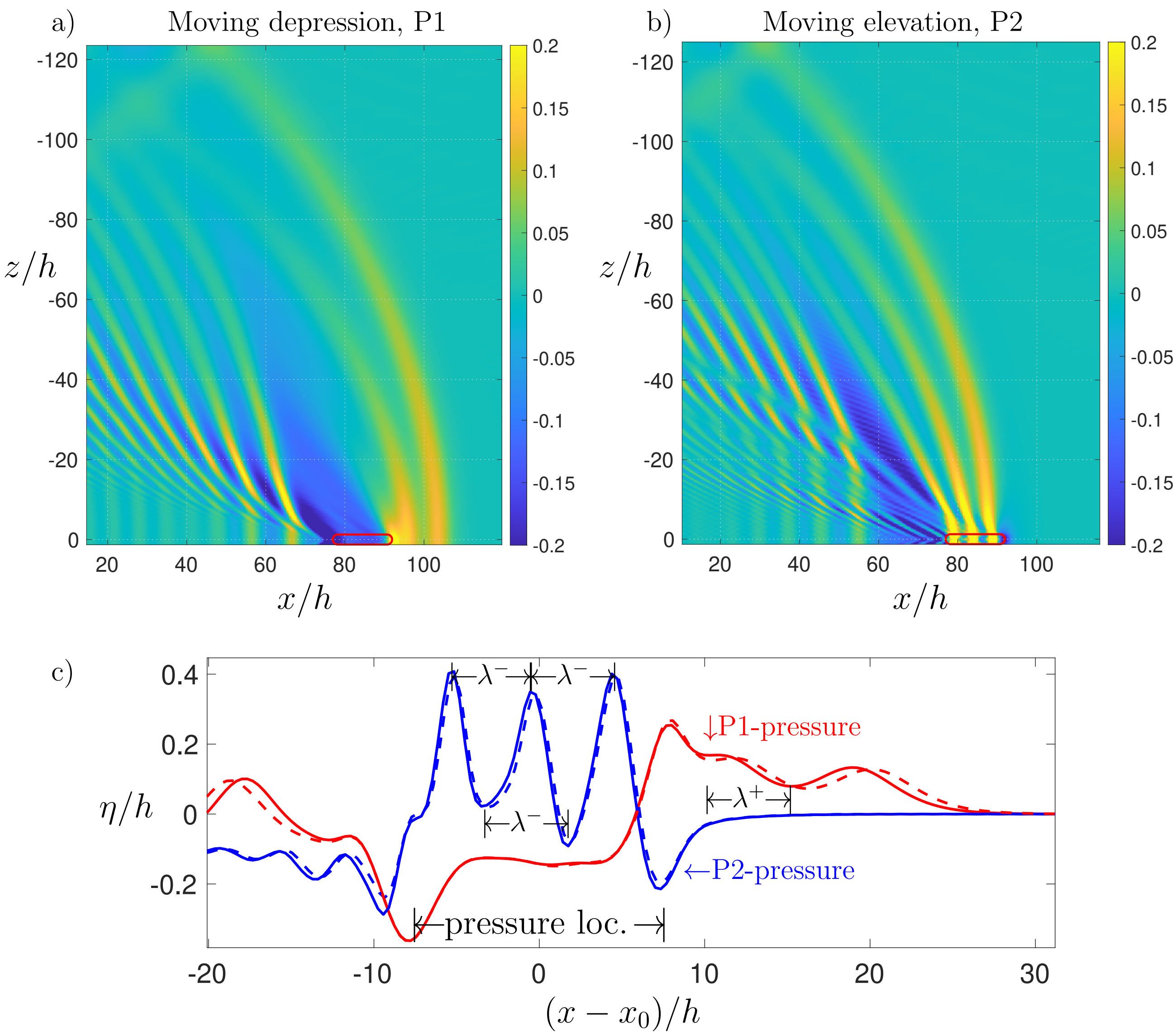

Figure 2: Elevation in color scale ($t = 200\sqrt{h/g}$) driven by moving a) high pressure, P1 (ship), b) low pressure, P2. The location of the pressure system is indicated by the red contour. c) Elevation along the x-axis for high pressure, P1 (red) and low pressure, P2 (blue). $t = 200\sqrt{h/g}$ (solid line) and $t = 220\sqrt{h/g}$ (dashed). Wavelengths λ^+ (λ^-) of the P1(P2) systems indicated. $Fr = 1$.

Figure 2a shows the upstream wave system as well as the downstream waves due to the (high-) pressure system, P1. Two upstream three-dimensional solitons are generated. The present fully dispersive and strongly nonlinear calculations generalise the asymptotic and long wave simulations by Lee and Grimshaw (1990) and Li and Sclavounos (2002), as well as other calculations referenced in these papers. Some of these calculations were made for rather long, wide and shallow pressure distributions fitting to the long wave regime.

Figure 2b shows the waves resulting from the inverted (low-) pressure system, P2. This artifice is used to illustrate of the dispersive contribution to the upstream wave generation of the P1-system. A depression is observed ahead of the P2-pressure. A short wave train with three crests is attached to the moving pressure. Figure 2c illustrates the elevation along the x-axis. The wave group generated by the P2-system, attached to the moving pressure, is characterised by a wave speed corresponding to $Fr = 1$. Moreover, a wavelength is clearly defined. We denote this by λ^-. The computations show that this wavelength, between the three crests and between the two troughs, is the same, where $\lambda^- \simeq 4.95h$. The corresponding wavenumber of $hk^- \simeq 1.27$ is in the intermediate depth range.

As regards the upstream waves due to the P1 system, the waves emerge from the bow wave. A trough to trough wave length (λ^+) of the wave, right upstream of the bow wave is defined (see figure 2c). This wavelength increases with time. However, at the inception, this trough to trough wave length is equally long as the wavelength attached to the P2-system (λ^-). In the calculation $\lambda^+ \simeq 4.83h$ at $t = 200\sqrt{h/g}$ while it is $\lambda^+ \simeq 5.89h$ at the later time $t = 220\sqrt{h/g}$. This implies that $\lambda^+ \simeq \lambda^-$ at the inception of the upstream wave generation. This illustrates the dispersive effect of the upstream generation of three-dimensional solitons at $Fr = 1$.

We note that the dispersive properties discussed here are very visible in calculations where the pressure (ship) is moving past a depth change, where the speed increases from subcritical to critical (calculations not shown). However, the wavelength attached to the moving pressure is more clearly defined by λ^- developing by the P2-system.

In the present simulations two curved upstream solitary waves were generated. The pressure system has moved a distance of 200 water depths corresponding to 2.8 km with $h = 14$ m. In reality the shoal (of $h = 14$ m) extends a few hundred meters.

4 References

Grue, J. (2017) Ship generated mini-tsunamis. J. Fluid Mech. 816, 142-166.
Lee, S.-J., and Grimshaw, R.H.J. (1990) Upstream-advancing waves generated by three-dimensional moving disturbances. Phys. Fluids A: Fluid Dynamics 2, 194.
Li, Y., and Sclavounos, P.D. (2002) Three-dimensional nonlinear solitary waves in shallow water generated by an advancing disturbance. J. Fluid Mech. 470, 383-410.
Torsvik, T., Soomere, T., Didenkulova, I., and Sheremet, A. (2015) Identification of ship wake structures by a time-frequency method. J. Fluid Mech. 765, 229-251.
Wu, T.Y. (1987) Generation of upstream advancing solitons by moving disturbances. J. Fluid Mech. 184: 75–99.